

Ku-band Reconfigurable MEMS Antenna on Silicon substrate

Ayan Karmakar¹, Amanpreet Kaur² and Kamaljeet Singh¹

¹MEMS Development Division, Semi-Conductor Laboratory (SCL), Mohali, Punjab.

²Student of Dept. of Electronics and Communication, Chitkara University, Himachal Pradesh.

ayanns@gmail.com

Abstract- This article presents design and fabrication methodology of Ku Band (linearly polarized) reconfigurable patch antenna. Both bulk and surface micromachining techniques are implemented on patch to have better RF performances. Reconfigurability is implemented by integrating shunt capacitive switch with microstrip patch antenna. Effect of feed mechanisms and role of micromachining on antenna parameters have been detailed here. Simulation was carried out for 675 μm high resistive Si-substrate with commercially available FEM based EM solver. A frequency drift of 200 MHz is achieved at Ku-band for the designed antenna.

Index Terms —Reconfigurable Antenna, Inset feed, quarterwave matching, micromachining.

I. INTRODUCTION

Modern communication system demand compact size, simpler topology and efficient microwave circuits which can be used for multiband applications. Tunable circuits are always preferred in wireless applications for multiplexing different channels/signals. MEMS technology is suitable in this respect offering various promising advantages compared to its counter parts, like-minimum insertion loss, less inter-modulation products, low volume, small size, etc. Designing front end antenna is a challenging task for a reconfigurable/adaptive system. Researchers are now engaging themselves to make use of RF MEMS switch for tuning single radiating elements to cater multiband operations [1-4].

The present work is based on designing an efficient Ku-band reconfigurable antenna. Reconfigurability is implemented by integrating shunt capacitive RF switch with electrostatic actuation. The designed antenna resonates at 14.5 GHz when switch is up state (air-gap = 3 μm) and at the down state of the switch, antenna is tuned at 14.3 GHz. Here, the switch acts as a variable two state capacitor, with capacitance ranging from fF to pF [5]. Further RF characteristics of the patch have been improved with micromachining technique. The design is based on 675 μm thick high resistive silicon substrate ($\rho > 8 \text{ K}\Omega\text{-cm}$, $\tan\delta = 0.01$). The designed antenna offers an input return loss of better than 23 dB, bandwidth of 844 MHz, 4.8 dB gain, 4.9 dB directivity, 20 dB FBR and around 97 % radiation efficiency for both of the targeted frequencies.

II. DESIGN DETAILS

Initially, we design conventional inset-feed microstrip patch antenna for 14.5 GHz on high resistive Si-substrate ($h = 675 \mu\text{m}$, $\tan\delta = 0.01$) taking the effective permittivity as follows [6-7]:

$$\epsilon_{r_{eff}} = \left[\frac{\epsilon_r + 1}{2} + \frac{\epsilon_r - 1}{2} \right] * \left[1 + \frac{12h}{w} \right]^{(-0.5)} \dots\dots\dots(1)$$

Where, ϵ_r is the dielectric constant of Si (11.8)

h = substrate height (675 μm)

w = width of the microstrip for 50 Ω line.

The physical parameters of the patch were evaluated by standard design equations [8-9]. For reconfigurability, capacitive shunt switch has been used. It acts as a two-state capacitor. The capacitance changes from 82 fF to 6 pF, while the state of the RF switch alters from Up to DOWN position. This capacitance ratio (C_{down}/C_{up}) dictates the figure of merit (FOM) of the switch. It can be further be enhanced with the use of high-k dielectric over the actuation pad. . In present case, 1500 \AA thick silicon nitride layer has been taken into consideration. The physical configuration of the RF switch has been freeze as per the foundry constraints. The physical and electrical design parameters of the RF switch is shown in Table-I.

In this work, both inset-feeding and the quadrature wave feed have been implemented in the patch. Then, at the radiating edge of the patch, notches are incorporated (along with T-shaped open circuited stub) over which switches are embedded. The position and dimension of the notches have been optimized by considering the surface current distribution of the patch with the aid of FEM based EM solver [10]. The schematic of the reconfigurable patch antenna with inset

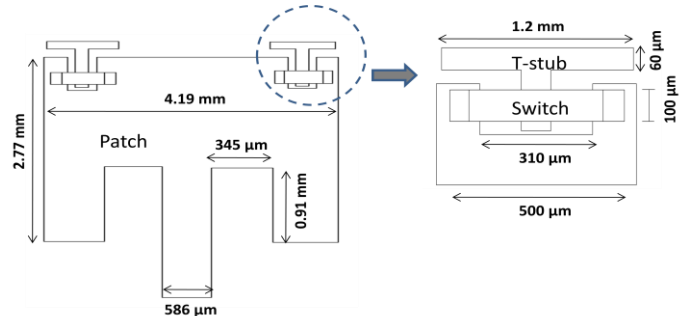


Fig.1: Reconfigurable patch antenna element
10-14 December 2013

TABLE I
RF SWITCH DIMENSIONS

Parameters	Values
Length of the switch membrane	310 μm
Width of the switch membrane	100 μm
Thickness of the switch membrane	0.5 μm
Pull-down voltage	30 V
Material used for Switch membrane	Gold
Initial Air-gap height	3 μm

TABLE II
COMPARATIVE STUDY OF THE VARIOUS DESIGNED ANTENNA VARIANTS

Antenna Parameters	Inset feed Patch antenna (Standard)	Quarter-Wave feed Patch Antenna	Reconfigurable inset feed antenna when	
			Switch UP (f = 14.5 GHz)	Switch DOWN (f = 14.3 GHz)
Return Loss(dB)	-24.93	-27.35	-23.75	-23.33
Bandwidth(MHz)	380.5	243.0	377.5	386.7
Directivity(dB)	3.11	1.78	2.68	2.65
Gain(dB)	2.78	1.18	2.78	2.35
Efficiency (%)	92.89	87.25	92.89	93.36
FBR(dB)	17.40	11.47	22.73	23.14

From the results depicted by Table-II, it is clear that though input matching is improved significantly in case of quarter-wave feeding, but the other antenna parameters degrades because of inherent narrow band characteristics of the input $\lambda/4$ line. All these degraded parameters can be significantly improved with the aid of micromachining[11]. Micromachining beneath the entire radiating patch is possible in case of $\lambda/4$ -fed antenna. As the feed line shouldn't be affected with micromachining effect, so inset-feeding doesn't serve the purpose well in this respect. There can be generation of unwanted spurious modes.

The bulk removal of the Si substrate is done practically by KOH etching at 80°C with the approximate etch rate of 1.1 $\mu\text{m}/\text{min}$. The dimensions of the micromachined patch dimension are calculated using the following equations [11]:

$$W = \frac{c}{\left((2 * f_r) * \left(\frac{\epsilon_{\text{reff}} + 1}{2} \right)^{\left(\frac{1}{2} \right)} \right)} \quad \dots\dots\dots(2)$$

$$L = \left[\frac{c}{(2 * f_r) * \sqrt{\epsilon_{\text{reff}}}} \right] \quad \dots\dots\dots(3)$$

Where, W= Width of the micromachined antenna,

L= Length of the microamchined antenna

f_r = resonant frequency

ϵ_{reff} = Effective dielectric constant of the substrate

c= Velocity of the light in vacuum

Taking the optimized membrane thickness as 30 μm , the length and width of patch over the cavity come out as 4.19 mm and 2.27 mm, respectively. The cross-sectional view of

the designed antenna is shown in Fig.2, whereas Fig.3 shows the 3D diagram of the designed antenna built in HFSS. It shows that the bulk micromachining is done beneath the patch only. And the switches are realized with surface micromachining. When the switch is in up-state, antenna radiates at 14.5 GHz and it tunes at 14.3 GHz while the state of the switch changes from up to down, Fig.4 shows it graphically. Table-III summarizes the RF performance of the reconfigurable antenna for two distinct switch states. It depicts that return loss, bandwidth, directivity, gain, radiation efficiency and finally front to back ratio of the bulk-micromachined quarter-wave fed antenna are far superior than its counterparts. Basically, bulk removal of high permittivity substrates like Silicon from the bottom portion of the radiating element make it almost loss less dielectric, which further enhance the bandwidth and gain parameters. As it is obvious, this design needs critical fabrication steps for realization.

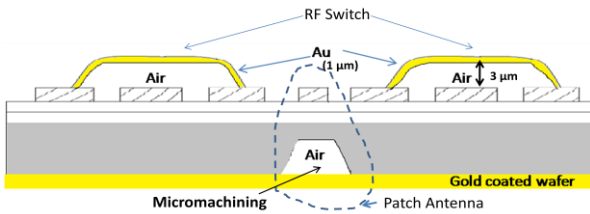


Fig.2: Cross-section view of the Reconfigurable Patch Antenna

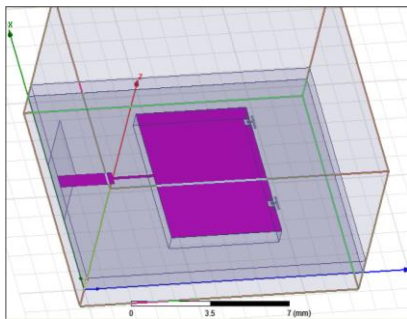


Fig.3: Bulk μmachined Quarter wave feed antenna

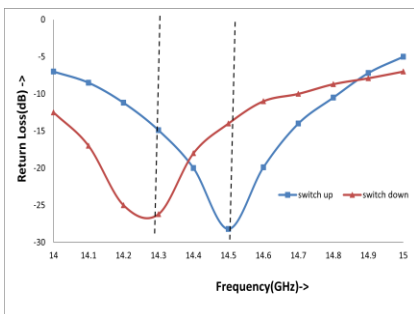


Fig.4: Return Loss of the designed reconfigurable antenna

The far field radiation pattern of the reconfigurable antenna is shown in Fig.5. It shows a stable directive pattern in the broadside fashion, consisting few numbers of grating/minor lobes.

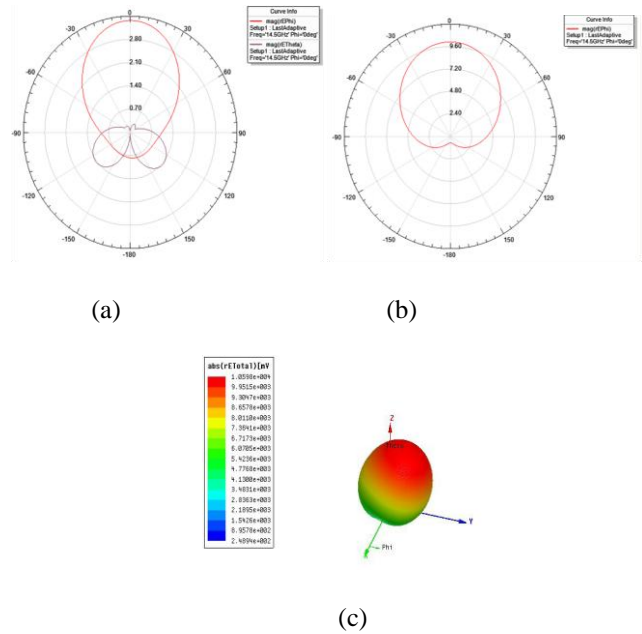


Figure-5: Radiation Pattern of the antenna when (a) Switch is up (b) when Switch is down (c) 3D pattern

CMOS/MEMS foundry. Proposed fabrication steps are detailed below:

- a) Starting material (High-Resistive Si of 675 μm thickness)
- b) Base oxide(500 Å) deposition in furnace
- c) PECVD Nitride deposition(1500 Å)
- d) Aluminium sputtering and patterning (1μm)
- e) Sacrificial oxide (BPSG) deposition (2.5μm) and patterning using MESA lithography.
- f) Lift off lithography and E-beam evaporation for 1 μm (for Gold deposition)
- g) Bulk-micromachining using KOH etching (30 μm membrane realization).
- h) Eutectic bonding of bottom-side gold coated wafer(Microstrip ground formation)
- i) Sacrificial oxide etching to realize the RF MEMS switch structure.

Due to process and equipment specs, inherent process deviations are expected resulting in variation of width, length and thickness of the device. These tolerance aspects are considered in simulations by utilizing sensitivity analysis. Metal thickness tolerance play minimal role as skin depth at 14.5 GHz is 0.67 μm.

Bulk-micromachining is one of the key process in MEMS technology. In realizing the micromachined antenna, the thickness of the membrane decides the effective permittivity o

the substrate, hence the bandwidth and radiation efficiency of the antenna are influenced.

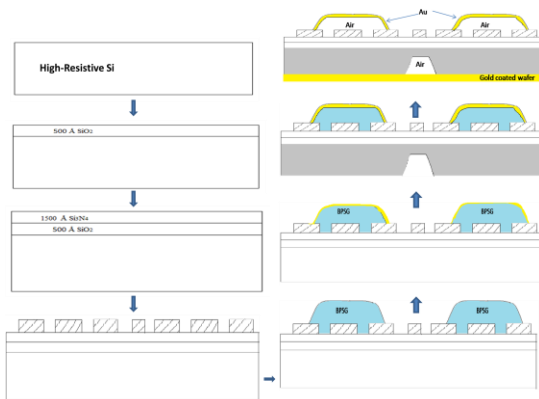


Fig.6 : Proposed fabrication steps of the micromachined reconfigurable patch antenna

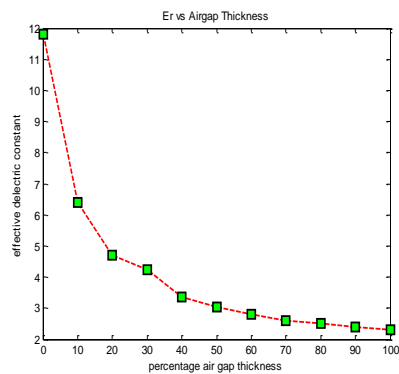


Fig.7: Variation of effective permittivity with Percentage of air-gap thickness

Fig.7 shows the variation of effective permittivity of the patch with membrane thickness. It depicts that, $30 \pm 4 \mu\text{m}$ membrane thickness is acceptable to achieve $\sim 95\%$ of air-cavity for the targeted antenna.

In the step(e) of Fig.6, the sacrificial oxide BPSG demand planarization, for better uniformity of switch membrane realization. For larger feature sizes of MEMS devices, multilevel planarization doesn't become much useful, leaving $\pm 0.5 \mu\text{m}$ variation in final product air-gap height. Air-gap height dictates the pull-down voltage of the RF switch. Pull-down voltage is one of the important parameter of the device.

Finally, the width variation of the transmission line is also taken care in this study. It shows that, $\pm 10 \mu\text{m}$ tolerance is acceptable for input 50Ω feed line, patch dimensions and T-shaped stub implementation. In CMOS foundry contact or proximity lithography offers almost accuracy in the order of used process technology dimensions. So, the mentioned tolerance level of the proposed design falls well below in the range of technology used.

IV. CONCLUSION

This article presents the design of a reconfigurable Ku-Band patch antenna using MEMS switch and the proposed fabrication process is compatible with standard CMOS foundry. Sensitivity analysis with the process tolerances have also been highlighted here. As per authors' knowledge, present work for the first time demonstrates the implementation of both bulk and surface micromachining in the realization of reconfigurable antenna on high permittivity substrate to achieve simultaneous bandwidth, gain, directivity and radiation efficiency optimally.

The circuit is under fabrication using our in-house facility.

REFERENCES

- [1] G. M. Rebeiz and J. B. Muldavin, "RF MEMS switches and switch circuits," IEEE Microwave Magazine, pp. 59-71, Dec. 2001.
- [2] Rainee N. Simons and Donghoon Chun and Linda P.B. Katehi, "Reconfigurable array antennas using Microelectromechanical systems (MEMS) actuators", NASA GRC report.
- [3] Rainee N. Simons, "Novel On -wafer Radiation Pattern Measurement technique for MEMS actuator based Reconfigurable patch Antennas", NASA GRC report-NASA/TM-2002-21816.
- [4] DeSignor, Jessica A., and Jayanti Venkataraman. "Reconfigurable Dual Frequency Microstrip Patch Antenna Using RF MEMS Switches." *IEEE Xplore*. May 2007. Web. 20 Sept. 2011.
- [5] A.Karmakar, K.Singh and K. Nagachenchaiah, "Electrostatic and electromechanical analysis of RF-MEMS capacitive type shunt switch" in Souvenir of National Conference on MEMS, Microsensors, Smart Materials, Structures and Systems[ISSS-MEMS-2007], November'2007, CEERI, Pilani.
- [6] K.C.Gupta, R. Garg, I. Bahl and P. Bhartia , "Microstripline and slotline", 2nd Edition, Artech House Publication,1996.
- [7] Pozar D.M. "Microwave Engineering", John Wiley and Sons Inc,New York,1998.
- [8] Pozar D.M, "Micro strip antennas", Proceedings of the IEEE,vol. 80,pp.79-91,1992.
- [9] Balanis C.A , "Antenna Theory :Analysis and Design", John Wiley and Sons Inc,New York,1997.
- [10] HFSS ver. 11, Ansoft Corporation.
- [11] Papapolymerou, Drayton, and Linda P. B. Katehi, "Micromachined Patch Antennas", IEEE Trans. Antennas and Propagations, vol. 46, no. 2, February 1998.

BIO-DATA OF AUTHORS

Ayan Karmakar received the B.Tech degree in Electronics & Communication Engineering from West Bengal University of Technology(WBUT), Kolkata, in 2005. In the year 2006, he joined ISRO as a Scientist. And, subsequently has been posted to SCL, Chandigarh in MEMS Development Division. His research interests include design & development of X-band and K-band passive microwave integrated circuits using silicon based MIC and RF-MEMS technology. E-mail: ayanns@gmail.com



Amanpreet Kaur, has obtained her B. Tech (ECE) degree from Chitkara University, Himachal Pradesh in 2013. She was doing the final year project in the MEMS Development Division of SCL, Chandigarh on reconfigurable RF devices. She joined Samsung Electronics in year 2013 as Quality Analyst and currently being posted in Samsung Research Institute, Noida.

E-Mail:
amansandhu2363@gmail.com



Kamaljeet Singh,FIETE,MIEEE has obtained M. Tech (Microwaves) from Delhi University in 1999 and PhD from Rajasthan University. He joined ISRO Satellite center, Bangalore in 1999 where he worked in the receiver division. From August 2006, he is working in MEMS area at SCL,Chandigarh.

E-Mail: kamaljs@scl.gov.in